Physics – Uspekhi **54** (5) 465 – 471 (2011)

REVIEWS OF TOPICAL PROBLEMS PACS numbers: **61. 72. – y**, **62.20. – x**, 81.30.Kf

The distribution of carbon in steels

Yu S Nechaev

DOI: 10.3367/UFNe.0181.201105b.0483

Contents

Abstract. The nature and characteristics of the way carbon present in steel is distributed spatially and over states may be related to quasichemical 'reactions' that lead to the formation in austenite (γ-Fe – C) and ferrite (α-Fe – C) of 'carbo-austenite' and 'carbo-ferrite molecules' (nanocomplexes) consisting, along with C atoms, of, respectively, γ-Fe or α-Fe and of octahedral γ- or α-interstitials. In this way, various aspects of the quasichemical dissolution and diffusion 'reactions' of carbon in the material can be determined, as can the quasichemical component of the martensite transformation (MT) mechanism in carbon steels.

1. Introduction

The study of the processes by which carbon and other interstitial impurities are distributed in steels is of great interest for understanding the observed properties of steels. There are two factors that should be considered in this context, along with usual diffusion: the chemical activity of carbon, and martensite transformations (MTs) (see, for example, Refs [1–4]) which steels undergo under cooling conditions and which initiate impurity redistribution processes. It is worthwhile noting that, as emphasized in Ref. [4], mechanisms that distribute and redistribute carbon atoms over a martensite lattice were the key preoccupation of G V Kurdyumov's last active years. This problem, also relevant to nitrogen atoms, is far from being solved and needs further investigation [2, 4, 5].

The present paper reviews available experimental and theoretical results on carbon arrangement and state in austenite, ferrite (interstitial solution of carbon in α-iron, a stable low-temperature phase), cementite (iron carbide, Fe_3C, the second stable low-temperature phase), and martensite. The paper uses analytical approaches and methods and results from thermodynamics and crystal chemistry [6–9] and compares and systematizes a large body of experimental and theoretical data to identify the mechanisms behind, patterns in, and characteristics of processes (phenomena) at the electronic, atomic, and nanostructural levels.

2. Arrangement and state of carbon in iron and steels

2.1 Carbon austenite: crystallochemical formula of carbon dissolution and diffusion reactions in γ-Fe

Carbon austenite is a face-centered cubic (fcc) solid solution of C in γ-Fe. According to the experimental data (reviewed in, for example, Refs [10, 11]), the partial solution enthalpy and the diffusion activation enthalpy (energy) of carbon in γ-Fe (carbon austenite) remain constant within the limits of experimental error bars or change only slightly over the wide (1 to 7 at.%) carbon concentrations typical of ideal or near-ideal solutions [10, 12].

On the other hand, as the same Refs [10, 11] also report, the thermodynamic activity and diffusion coefficients of carbon in austenite depend significantly on the impurity (C) concentration, which disagrees with observations in ideal solutions [10, 12].

Yu S Nechaev G V Kurdyumov Institute of Metal Science and Physics, State Research Centre of the Russian Federation
'I P Bardin Central Research Institute of Ferrous Metallurgy',
2-ya Baumanskaya ul. 9/23, 105005 Moscow, Russian Federation
Tel./Fax (7-495) 777 93 50
E-mail: yuri1939@inbox.ru

Received 15 August 2010, revised 18 September 2010
Uspekhi Fizicheskikh Nauk **181** (5) 483 – 490 (2011)
DOI: 10.3367/UFNr.0181.201105b.0483
Translated by E G Strel'chenko; edited by A Radzig

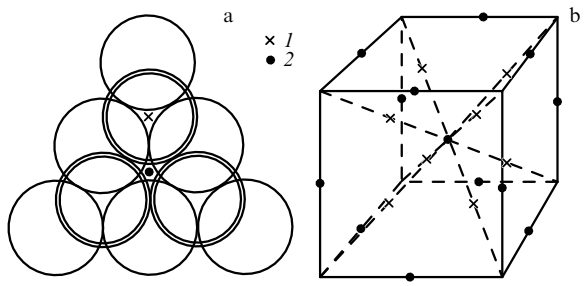

Figure 1. (a) Tetrahedral (*1*) and octahedral (*2*) interstices (voids or pores) in a two-layer closest-packed lattice. Upper layer atoms are shown as doubled circles. Each octahedral void (pore) resides between six tangent 'balls', i.e., between structurally equivalent atoms that are the void's (pore's) nearest neighbors. (b) Positions of tetrahedral (*1*) and octahedral (*2*) interstices (voids, pores) in the fcc lattice. Atoms are not shown. There are two tetrahedral pores and one octahedral pore for each atom of the fcc lattice.

A similar situation occurs for nitrogen in γ-Fe (nitrogen austenite, with up to 10 at.% N) [10, 11].

A statistical thermodynamic analysis of the experimental results produced in Refs [10, 11] relies on modeling the interstitial solutions of carbon (or nitrogen) atoms in an fcc structure (Fig. 1 [13]) ('interstitial' referring to octahedral interstices, OI_γ) and uses an additional empirical hypothesis to explain the above-mentioned deviations from the behavior of ideal solutions [10]. The hypothesis is that each carbon (or nitrogen) atom occupying an austenite OI_γ creates conditions which, even for highly diluted solutions, prevent a certain number ($n^*_{C\gamma} = 3-5$) of neighboring OI_γ from being occupied by other carbon (or nitrogen) atoms, the number in question being OI_γ for carbon [10, 11] and $n^*_{N\gamma} = 3-12$ for nitrogen [10, 11].

It should be noted here that neither X-ray nor neutron diffraction studies [14] have revealed any deviation from a random (chaotic) distribution of carbon atoms in the austenite lattice. This is believed [10] to be possibly due to both the low concentration of carbon and the insufficiently sensitive methods of investigation [14]. On the other hand, Mössbauer spectroscopy data on austenite [15, 16] indicate that the number of iron atoms with a single C neighbor is larger than for a random distribution. In addition, the Mössbauer spectra of austenite show no or weak lines from iron atoms with two carbon neighbors [15, 16], implying that the $n^*_{C\gamma}$ (or $n^*_{N\gamma}$) $\geqslant 3$ hypothesis [10] is compatible to independent structural data [14–16].

As noted in Ref. [17, p. 69], the distribution of carbon atoms over OI_γ's in an austenite lattice is not strictly statistical because when one carbon atom is introduced into one of the OI_γ's, the electron density is redistributed locally, thus preventing the occupation of the nearest OI_γ's. Such a local state formed in the nearest neighborhood of each carbon atom dissolved in austenite is a kind of an 'island' where the covalent bonds of the carbon atom with the six nearest (structurally equivalent) iron atoms manifest themselves (see Fig. 1).

This is in agreement with theoretical data [18] on local electronic structures and covalent bonds of interstitial impurities (C, N) in austenite. According to these data, covalent σ bonds for each carbon (or nitrogen) atom in austenite (γ-Fe – C or γ-Fe – N) mainly manifest themselves locally within the first coordination sphere of the fcc structure, thus pointing to six nearest structurally equivalent iron atoms (see Fig. 1).

It is worthwhile noting that such a local state was conjectured ([17], p. 70]) to exist for a carbon atom in an octahedral interstice in iron carbide Fe_3C (cementite): a carbon atom captures two valence electrons of an iron atom and becomes an anion C^{2-}, in so doing forming six covalent bonds with iron ions occupying octahedron vertices. Later work ([17], p. 71) showed that covalent bonds formed in Fe_3C by four valence electrons of each carbon atom occupying a prismatic interstice and by 3d electrons of the four nearest iron atoms are localized in (metallically bonded) layers of prismatic structural elements.

Because in the fcc lattice there is one OI_γ per γ-Fe atom [13], covalent bonds that form between a carbon atom introduced in one of the OI_γ's and six nearest structurally equivalent iron atoms clearly 'poison' the five nearest OI_γ's, which means that $n^*_{C\gamma} = 5$. In a sense, what we have is an intercalated (absorbed) 'carbo-austenite molecule' of the γ-$Fe_6C(OI_\gamma)_6$ type with spherical symmetry with respect to the coordinate axes of the fcc lattice of γ-Fe (see Fig. 1).

In this picture, then, one carbon atom appears to 'occupy' six structurally equivalent OI_γ's that correspond to one absorption center for an impurity (C) atom in the fcc lattice of γ-Fe, and the quantity $1/(n^*_{C\gamma}+1)$ characterizes the number of moles of such absorption centers in a mole of OI_γs or in a mole of γ-Fe.

If absorbed carbo-austenite γ-$Fe_6C(OI_\gamma)_6$ molecules interact negligibly between themselves, then their thermodynamic activity ($a_{C\gamma}$) in austenite is described to good approximation by the Langmuir–McLin sorption isotherm (Fermi type distribution [19]), giving

$$a_{C\gamma} = \frac{P_{C\gamma}}{P^0_{C\gamma}} = \frac{(1+n^*_{C\gamma})\,X_{C\gamma}}{1-(2+n^*_{C\gamma})\,X_{C\gamma}}\,, \tag{1}$$

where $X_{C\gamma} = n_{C\gamma}/(1+n_{C\gamma})$ is the atomic fraction of absorbed carbon, $n_{C\gamma}$ is the number of the moles of carbon absorbed by one mole of austenite, and $P_{C\gamma}$, $P^0_{C\gamma}$ are equilibrium and standard carbon vapor pressures, respectively, above the austenite.

For $n^*_{C\gamma} = 5$, this yields

$$a_{C\gamma} = \frac{6X_{C\gamma}}{1-7X_{C\gamma}}\,, \tag{1a}$$

with the concentration $X^0_{C\gamma} = 1/13 \approx 7.7$ at.% and its associated $P^0_{C\gamma}$ corresponding to the standard state ($a^0_{C\gamma} = 1$) for carbon dissolved in the austenite lattice (i.e., for the crystallochemical dissolution reaction at the temperature considered).

Clearly, the choice of the standard state determines the standard changes of enthalpy (ΔH) and nonconfigurational entropy (ΔS) for the dissolution reaction, which determine, in turn, the equilibrium constant $K = \exp(\Delta S/RT)\times \exp(-\Delta H/RT)$ for this reaction [19].

The 'chemical' diffusion coefficient of absorbed carbon in austenite ($D_{C\gamma}$) is well known to be [12]

$$D_{C\gamma} = D_{0C\gamma}\exp\left(-\frac{Q_{C\gamma}}{RT}\right)\frac{\mathrm{d}\ln a_{C\gamma}}{\mathrm{d}\ln X_{C\gamma}}\,, \tag{2}$$

$$D_{C\gamma} = D_{0C\gamma}\,\frac{\exp(-Q_{C\gamma}/RT)}{1-7X_{C\gamma}}\,, \tag{2a}$$

where the pre-exponential factor $D_{0C\gamma}$ is frequency and entropy dependent, $Q_{C\gamma}$ is the diffusion activation energy

Table 1. Carbon solubility in undoped austenite (γ-Fe) from the analysis of experimental data of Refs [20–22] using expression (1).

Dissolution reactions	References	T, K	$n^*_{C\gamma}$
$CH_4(gas) \Longleftrightarrow [C]_{\gamma\text{-Fe}} + 2H_2(gas)$	[21]	1073	3.6 ± 0.2
$CH_4(gas) \Longleftrightarrow [C]_{\gamma\text{-Fe}} + 2H_2(gas)$	[21]	1273	4.2 ± 0.8
$2CO(gas) \Longleftrightarrow [C]_{\gamma\text{-Fe}} + CO_2(gas)$	[21]	1073	5.3 ± 0.2
$2CO(gas) \Longleftrightarrow [C]_{\gamma\text{-Fe}} + CO_2(gas)$	[21]	1273	4.8 ± 0.2
$2CO(gas) \Longleftrightarrow [C]_{\gamma\text{-Fe}} + CO_2(gas)$	[21]	1473	4.9 ± 0.5
$2CO(gas) \Longleftrightarrow [C]_{\gamma\text{-Fe}} + CO_2(gas)$	[22]	1173	5.3 ± 0.3
$2CO(gas) \Longleftrightarrow [C]_{\gamma\text{-Fe}} + CO_2(gas)$	[22]	1273	4.8 ± 0.2
$2CO(gas) \Longleftrightarrow [C]_{\gamma\text{-Fe}} + CO_2(gas)$	[22]	1573	5.0 ± 0.3

(enthalpy), R is the universal gas constant, and T is the absolute temperature. The quantity $d\ln a_{C\gamma}/d\ln X_{C\gamma} = d\ln P_{C\gamma}/d\ln X_{C\gamma}$ is clearly independent of the particular choice of the standard state for carbon in austenite ($P^0_{C\gamma} \approx$ const) and can be derived from experimental data on the concentration dependence of the diffusion coefficient [11].

Table 1 presents the experimental values of $n^*_{C\gamma}$ obtained using Eqn (1) from experimental data [20–22] on the solubility of carbon from the gaseous mixtures $CH_4(gas)/H_2(gas)$ or $CO(gas)/CO_2(gas)$ at different temperatures and pressures in undoped austenite (γ-Fe).

Averaging the listed values yields $n^*_{C\gamma} = 4.7 \pm 0.4$, i.e., $n^*_{C\gamma} \approx 5$, which confirms the validity of expression (1a) and is consistent with the crystallochemical aspects discussed above.

Similarly, from solubility data [23–26] on nitrogen in austenite (γ-Fe), one finds $n^*_{N\gamma} = 7.1 \pm 0.6$ — an experimental result which corresponds to the (clearly nonspherically symmetric) molecule γ-$Fe_8N(OI_\gamma)_8$ (see Fig. 1) and which needs further consideration.

It appears reasonable to give consideration to Mössbauer and other data [27, 28] on carbon clusterization (stratification) in γ-Fe under certain conditions, which clearly points to considerable negative interaction energy between carbon atoms [19], and so implies attraction between carbo-austenite γ-$Fe_6C(OI_\gamma)_6$ molecules.

To take into account this (relatively weak) interaction between absorbed γ-$Fe_6C(OI_\gamma)_6$ molecules, the Fowler-Guggenheim sorption isotherm [19] can serve as an approximation or a model, giving the following expression for the thermodynamic activity of carbon ($a_{C\gamma}$) in austenite (for $n^*_{C\gamma} = 5$):

$$a_{C\gamma} = \frac{6X_{C\gamma}}{1 - 7X_{C\gamma}} \exp\left\{\frac{\varepsilon\left[(13X_{C\gamma} - 1)/(1 - X_{C\gamma})\right]}{RT}\right\}, \quad (3)$$

where ε is the interaction energy between γ-$Fe_6C(OI_\gamma)_6$ molecules in austenite.

The effective chemical diffusion coefficient of carbon in austenite ($D^*_{C\gamma}$) is given by the expressions

$$D^*_{C\gamma} \approx D^*_{0C\gamma} \exp\left(-\frac{Q^*_{C\gamma}}{RT}\right), \quad (4)$$

$$D^*_{0C\gamma} \approx D_{0C\gamma}\left(\frac{12\varepsilon X_{C\gamma}}{RT(1 - X_{C\gamma})^2} + \frac{1}{1 - 7X_{C\gamma}}\right), \quad (5)$$

$$Q^*_{C\gamma} \approx Q_{C\gamma} + \Delta\varepsilon X_{C\gamma} \approx Q_{C\gamma}, \quad (6)$$

where the effective pre-exponential factor $D^*_{0C\gamma}$ is frequency and entropy dependent, $Q^*_{C\gamma}$ is the effective diffusion activation energy, and $\Delta\varepsilon$ is the energy parameter described in Ref. [12].

Using Eqns (3)–(6) to analyze experimental data [10, 11, 21, 22, 29–31] on the solubility and diffusion of carbon in γ-Fe yields the following: (1) the interaction energy between γ-$Fe_6C(OI_\gamma)_6$ molecules in the austenite lattice, $\varepsilon \approx -2$ kJ mol^{-1} (-0.02 eV), which corresponds to the relatively weak attraction between them that can lead to clusterization [19], (2) the energy parameter $\Delta\varepsilon \approx -100$ kJ mol^{-1}, and (3) the standard changes in enthalpy ($\Delta H_4 \approx 260$ kJ mol^{-1}) and nonconfigurational entropy ($\Delta S_4 \approx 28R$) for the dissociative dissolution reaction, see Eqn (10) below, of CH_4(gas) in austenite (at 1073 K and 1273 K).

In light of the above, the equations (crystallochemical formulas) for the reactions of dissolution ($CH_4(gas) \Leftrightarrow [C]_{\gamma\text{-Fe}} + 2H_2(gas)$) and diffusion of C in γ-Fe can be written in the form

$$CH_4(gas) \Rightarrow C(graphite) + 2H_2(gas), \quad (\Delta H_1, \Delta S_1), \quad (7)$$

$$C(graphite) \Rightarrow C(gas), \quad (\Delta H_2, \Delta S_2), \quad (8)$$

$$C(gas) + 6\gamma\text{-Fe} + 6OM_\gamma \Rightarrow \gamma\text{-}Fe_6C(OM_\gamma)_6, \quad (\Delta H_3, \Delta S_3), \quad (9)$$

$$CH_4(gas) + 6\gamma\text{-Fe} + 6OM_\gamma \Rightarrow \gamma\text{-}Fe_6C(OM_\gamma)_6 + 2H_2(gas), \quad (\Delta H_4, \Delta S_4), \quad (10)$$

$$\Delta H_3 = \Delta H_4 - \Delta H_1 - \Delta H_2, \quad \Delta S_3 = \Delta S_4 - \Delta S_1 - \Delta S_2, \quad (11)$$

$$\gamma\text{-}Fe_6C(OM_\gamma)_6 + 6\gamma\text{-}Fe' + 6OM'_\gamma \Rightarrow 6\gamma\text{-Fe} + 6OM_\gamma + \gamma\text{-}Fe'_6C(OM'_\gamma)_6, \quad (12)$$

$$Q_{C\gamma} \approx -0.3\Delta H_3, \quad \Delta S_{C\gamma} \approx -0.3\Delta S_3, \quad (13)$$

where ΔH_{1-4} and ΔS_{1-4} are the standard changes in enthalpy and entropy for the corresponding reactions, $\Delta S_{C\gamma}$ is the nonconfigurational diffusion activation entropy as determined from the experimental values of $D_{0C\gamma}$ (Ref. [11] and some others), Eqn (10) is the equation (crystallochemical formula) for the dissociative dissolution of CH_4(gas) in γ-Fe, and Eqn (12) is the same for carbon diffusion in austenite.

The known experimental values of ΔH_1, ΔH_2, ΔH_4, ΔS_1, ΔS_2 and ΔS_4 yield, using Eqn (11), the formation energy and formation entropy for γ-$Fe_6C(OI_\gamma)_6$ molecules in austenite (from C(gas) and γ-Fe), $\Delta H_3 \approx -5.8$ eV, and $\Delta S_3 \approx -7.5R$, respectively, which characterize the bonding of absorbed carbon to austenite.

It should be emphasized that the known experimental values of the diffusion activation energy (enthalpy) $Q_{C\gamma}$ and the nonconfigurational entropy (from $D_{0C\gamma}$) of carbon in austenite [11, 29–31] are accounted for satisfactorily in a model in which the well-known idea of covalent bonds being redistributed during transition state formation is applied to the diffusive hopping of a carbon atom from an occupied absorption 'center' to a neighboring free absorption center where covalent bonds manifest themselves [see the crystallochemical formula (12)].

The activation energy $Q_{C\gamma}$ of the diffusion process can, in this situation, be on the order of 20–30% of the broken bond energy $-\Delta H_3$, formula (13), which is typical of the corresponding chemical reactions [32]. A similar situation can also occur for the activation energy $\Delta S_{C\gamma}$ of the process, see formula (13).

This interpretation of the diffusion activation energy of carbon in austenite is consistent with theoretical data [18] on the localization of covalent σ bonds (γ-Fe – C) within the first coordination sphere of the fcc structure of γ-Fe.

The discussion above shows that the local state and arrangement of C in austenite can be thought of in terms of 'intercalated' (absorbed), spherically symmetric γ-$Fe_6C(OI_\gamma)_6$ type molecules weakly interacting with one another (attraction that leads, under certain conditions, to clusterization), with one C atom 'occupying' six structurally equivalent octahedral interstices (OI_γ) which correspond to one 'absorption center' of the impurity (C) atom in the fcc lattice of γ-Fe (see Fig. 1).

2.2 Ferrite: local state, arrangement, and dissolution and diffusion reaction formulas for C in α-Fe

A discussion similar to that of Section 2.1 reveals that the local state and arrangement of carbon in ferrite (body-centered cubic or bcc solid solution of C in α-Fe) can be thought of in terms of intercalated (absorbed) dumbbell-shaped, cylindrically symmetric α-$Fe_2C(OI_\alpha)_6$ type molecules weakly interacting with one another (analysis of experimental data identifies this interaction as repulsion).

In this picture, a carbon atom 'occupies' six octahedral interstices (OI_α) corresponding to one absorption center of an impurity (C) atom in the bcc lattice (Fig. 2 [13]).

The crystallochemical formulas for the dissolution and diffusion of C in ferrite, i.e., for dumbbell-shaped α-$Fe_2C(OI_\alpha)_6$ molecules, are similar to expressions like (1)–(13) for spherical γ-$Fe_6C(OI_\gamma)_6$ molecules.

2.3 Martensite

The local state, arrangement, and dissolution 'formulas' of C in a martensite lattice (α^*-Fe, body-centered tetragonal or bct stressed nanostructure) are similar to those for ferrite (α-Fe), but with a higher level of elastic stress in the material and with dumbbell-shaped α^*-$Fe_2C(OI_{\alpha^*})_6$ molecules preferentially oriented along the tetragonal axis due to their interaction with one another (at a sufficiently high impurity concentration), the interaction likely being repulsion between the saturated bonds [32] and/or of elastic origin (that between elastic dipoles [33]).

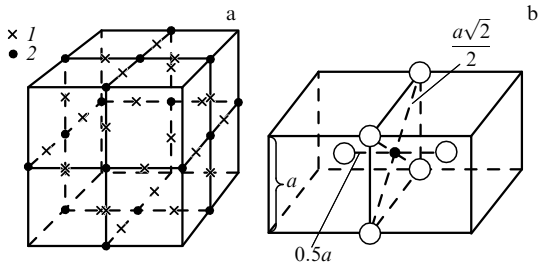

Figure 2. (a) Positions of tetrahedral (*1*) and octahedral (*2*) voids (pores) in the bcc lattice. Atoms are not shown. There are six tetrahedral and three octahedral voids (pores) for each atom of the bcc lattice. (b) Six atoms surrounding an octahedral pore in the bcc lattice; two of them are much closer than the others and are structurally equivalent nearest neighbors of the octahedral pore.

3. Crystallochemical correspondence between carbon distributions in the austenite and martensite of carbon steels

The data in Refs [1–4] together with the results discussed in Sections 2.1–2.3 suggest for carbon steels the following relation [crystallochemical reaction inherent in martensite transformation (MT)]:

$$n\gamma\text{-}Fe_6C(OM_\gamma)_6 \Rightarrow n\left[\alpha^*\text{-}Fe_2C(OM_{\alpha^*})_6\right] + 4n\alpha^*\text{-}Fe + 12n(OM_{\alpha^*})\,, \tag{14}$$

where $n \gg 1$ is the number of dumbbell-shaped α^*-$Fe_2C(OI_{\alpha^*})_6$ molecules that are ordered (i.e., oriented along the tetragonal axis) in certain regions of the material (identified in structural, dimensional, crystallographic, and other terms), in which cooling (quenching) causes the spherical γ-$Fe_6C(OI_\gamma)_6$ molecules to cluster prior to the MT.

Expression (14) implies that in certain regions of the material, with a size on the order of the critical size for the start of the MT, clusters comprising n spherical γ-$Fe_6C(OI_\gamma)_6$ molecules can form new clusters consisting of n dumbbell-shaped α^*-$Fe_2C(OI_{\alpha^*})_6$ molecules (elastic dipoles or compressed nanosprings) oriented along the tetragonal axis ($4n$ neighboring α^*-Fe atoms and $12n$ OI_{α^*}s also form).

In this process, apparently, local covalent Fe–C σ bonds and iron atoms are redistributed in a certain way, giving rise, due to the energy of the quasichemical reaction (14), to the high local stresses [34, 35] necessary for shear MT deformation to occur in the material. This can be considered as the quasichemical, or crystallochemical, component of the MT mechanism in carbon steels. There is also reason to believe that for other systems with MT, other, case-relevant elastic dipoles should be involved [33].

4. Anomalous (diffusion) carbon redistribution toward dislocations during the high-rate deformation of carbon steels in martensite transformations

The analysis [9] of experimental data (Fig. 3) reveals that in carbon steel subject to high-rate MT deformation a concomitant process initiated by the martensite transformation may occur, namely, the anomalous diffusion-assisted redistribution of carbon atoms from the martensite lattice toward dislocations that form with density $\rho_\perp$ in the material (at separations on the order of $\rho_\perp^{-1/2} \approx 10$ nm).

Clearly, the diffusion time is close (by order of magnitude) to the MT time τ_{MT} which can (in light of Refs [1–4, 35] be estimated as

$$\tau_{MT} \approx \frac{L_{gr}}{v_s} \approx 10^{-8} - 10^{-9}\ \text{s}, \tag{15}$$

where L_{gr} is the size of the original austenite grains, and v_s is the speed of sound in the metal.

From this it follows that the rate of MT deformation may be estimated as

$$\varepsilon' \approx \frac{\delta}{L_{gr}\tau_{MT}} \approx 10^3 - 10^4\ \text{s}^{-1}, \tag{16}$$

where $\delta \approx 10^{-1}$ nm is the displacement of iron atoms in the MT [1–4, 35].

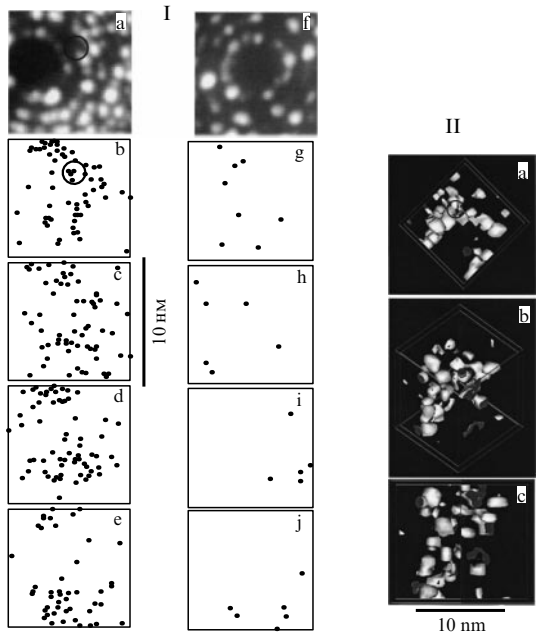

Figure 3. (I) ECOPoSAP [34] results in martensite regions (a–e) immediately above and (f–j) outside of a dislocation. The ionic force microphotographs of the analyzed areas (a) and (f) were obtained in He at 12 kV and 50 K. Four successive sections (b–e) and (g–j), each containing five atomic planes, were analyzed. In each case, the analyzed region was 10 ± 1.5 nm in width. Black circles in (a) and (b) show original dislocation positions. (II) ECOPoSAP [34] results in martensite regions immediately above a dislocation. Shown are isoconcentration (4 at.% C) surfaces in the S atmosphere for three different positions (angles) of observation. The width of the analyzed region is 10 ± 1.5 nm, and the depth of analysis reaches ~ 4 nm. The dislocation localization is shown by a dark circle in (I). Carbon content in original austenite is 0.85 at.%, the average density of dislocations in martensite is $\rho_\perp \approx 3 \times 10^{11}$ cm^{-2}, and the average separation between them is $\rho_\perp^{-1/2} \approx 18$ nm. (Taken from analytical review [9].)

The carbon diffusion coefficient towards dislocations in the MT can be estimated as follows:

$$D_C^* \approx (\rho_\perp \tau_{MT})^{-1} \approx 10^{-3} - 10^{-4} \text{ cm}^2 \text{ s}^{-1}, \tag{17}$$

which is in agreement with known experimental data on diffusion anomalies at high-rate (pulsed) deformation of metals [36, 37] and corresponds to a craudion type mechanism [38] (for such 'molecules', not for individual carbon atoms).

Similar values of deformation rates and diffusion coefficients are obtained, for example, for a metal compressed by a pulsed magnetic field [37].

Normal diffusion-assisted dislocation-directed post-deformation redistribution of carbon (with a diffusion coefficient $D_C \approx 3 \times 10^{-17}$ cm^2 s^{-1}) in martensite at room temperature was considered in Ref. [9] using data from Ref. [34] (see Fig. 3), the term post-deformation referring to the period lasting from the MT termination until the equilibrium carbon concentration (~ 0.17 at.%) with respect to carbide-like nanosegregations (adsorbed nanophase on dislocations) is attained in the stressed martensite lattice.

The point to emphasize here is that the anomalous diffusion coefficient of carbon (D_C^*) in martensite in the MT is 12–13 orders of magnitude larger than its normal post-MT room temperature counterpart (D_C).

5. On strengthening mechanisms and superplasticity manifestations in metal materials undergoing martensite transformation

As noted in recent monograph [2], any metal material capable of martensite transformations exhibits superplasticity.

The same Ref. [2] indicates that under certain conditions the interaction of a deformation with an MT can lead to a significant increase in plastic deformation, followed by the destruction of the material (so-called transformation-induced plasticity). In common materials, deformation leads, on the one hand, to increased strength and, on the other hand, to decreased plasticity.

It is found [2] that in alloys with a metastable austenite, deformation accompanied by the formation of martensite leads, in the temperature interval near the martensite point, to increased strength and, simultaneously, to a higher plasticity due to the appearance of martensite deformation.

There are reasons to believe [9, 34, 39, 40] that in many cases strengthening is, to a large extent, due to the high density of dislocations that are decorated, i.e., fixed by carbide-like nanosegregations (see Fig. 3) — a fact which is usually left out of discussions [2].

On the other hand, it appears to be necessary, when considering the superplasticity of transformation (MT), to take into account, as in the case of structural superplasticity, the possibility of deformation (dislocation-related) quasi-melting of part of the grain boundaries and phase interfaces in the material [9] — a fact which is also usually ignored [2].

6. Discussion

The first point to emphasize (in relation to the discussion on Refs [41, 42]) is that expressions (1a), (2a) (and their next better approximations (3)–(6)) obtained in the present paper are of the nature of an indirect experiment and are conceptually and methodologically significant because in their derivation (within the combined framework of thermodynamics and crystal chemistry) the following known data (together with the results of their analysis) were used:

(1) High-temperature and /or low-impurity-concentration data [14–16] on the near chaotic distribution of carbon atoms in the fcc lattice formed by octahedral interstices (OI_γs) in austenite (γ-Fe) that corresponds to the thermodynamic model of the lattice gas of interstitial impurities in the OI_γ-lattice (see review [10]).

(2) Evidence [10, 11, 20–22, 30] that, whereas the partial dissolution enthalpy and diffusion activation energy of carbon vary little or not at all with concentration, its thermodynamic activity coefficient and diffusion coefficient in the OI_γ lattice of austenite (γ-Fe) vary strongly with concentration. This fits with the ideal lattice gas model in which some configurations are 'excluded' [10], which is typical of the Langmuir–McLin sorption isotherm or of a Fermi type distribution (when Fermi type combinatorics are used). Notice that configuration exclusion in the distribution of carbon atoms (of an ideal lattice gas) over the OI_γs are obviously due to the properties of the local states near each impurity [17, 18] rather than due to the Pauli exclusion principle, as is the case for the ideal gas of fermions. A treatment of the Langmuir–McLin isotherm as a Fermi distribution analog (in relation to Cottrell clouds) is given, for example, in Ref. [43], in which an analog of the Fermi energy is also introduced.

(3) Results of processing data from Refs [10, 11, 20–22, 30] using expressions (1a) and (2a), which show unambiguously that one carbon atom in the OI_γ-lattice in austenite occupies (using the terminology and framework of Fermi type combinatorics) a cell of six octahedral interstices ($n^*_{C\gamma} + 1$), to which correspond six iron atoms in the austenite lattice (see Fig. 1). This suggests that all six iron atoms (the nearest impurity neighbors) in the first coordination sphere of each carbon atom dissolved (absorbed) in the austenite and occupying one of the OI_γs are excluded or 'poisoned', as far as the absorption of other carbon atoms is concerned. Thus, in the next higher approximation [expressions (3)–(6)], which includes some amount of interaction between carbon atoms dissolved in austenite, only the first coordination sphere can — and must — be considered. Results obtained in Refs [44–46] demonstrate that the thermodynamic properties of carbon in austenite are adequately determined by the interaction with the neighboring iron atoms only in the first coordination sphere of the impurity (in the framework of the quasichemical pairwise interaction model). A further point to note is that the second and even third coordination spheres considered in some work for an impurity in austenite overlap for real (up to 8 at.%) carbon concentrations, which is clearly inconsistent with an adequate determination of the thermodynamic activity of an impurity within the quasichemical model of pairwise interactions [32].

(4) The data of Ref. [18] on the local electronic structures and covalent bonds of interstitial (C) impurities in austenite (γ-Fe), which are mainly localized within the first coordination sphere. There are reasons [18, 32] to believe that it is only such short-range and relatively strong covalent σ bonds that can ensure the 'poisoning' of six iron atoms in austenite in precisely the first coordination sphere of the dissolved carbon atom.

(5) The data of Refs [27, 28] on the clusterization (stratification) of carbon atoms in γ-Fe (under certain conditions) and on the lack of their ordering in ordered alloys of the types Fe_4C, Fe_6C, etc. (in contrast to nitrogen, whose atoms order themselves into structures like Fe_8N ($Fe_{16}N_2$), etc. in austenite, according to some studies).

(6) Results of processing data from Refs [10, 11, 20–22, 29–31] using expressions (3)–(6), which provide the interaction energy between dissolved carbon atoms [γ-$Fe_6C(OI_\gamma)_6$ molecules] in the austenite lattice ($\varepsilon \approx -0.02$ eV), which corresponds to their relatively weak attraction capable of giving rise to clusterization (stratification) of the atoms (molecules).

(7) Data from Ref. [47] on local electron density redistribution for the 3d orbitals of iron atoms, which are the nearest neighbors (first coordination sphere) of austenite-dissolved carbon atoms and which exhibit, both in austenite and martensite, the properties of positively charged ions, i.e., cations. The data of Ref. [47] on the formation of strong covalent σ bonds in martensite between a carbon atom and two iron atoms which are the nearest neighbors to the impurity along the *c*-axis — that is, on the formation of an Fe_2C complex oriented either along the Fe_2-dipole distortion or along the Fe_2-dipole which corresponds to the d^2_Z orbital. The data of Ref. [47] agree with those of Ref. [33] on elastic Fe_2C-dipoles in ferrite.

(8) The data of Refs [48, 49] implying the possible formation of an ordered Fe_4C_x ($x < 1$) phase during the martensite tempering. The data of Refs [50–53] indicate that, as martensite ages, the clusterization, ordering, and segregation of carbon is possible, in particular, on grain boundaries and other lattice defects [53].

In light of the discussion above, it seems relevant that the following aspects of the problem of carbon distribution in steels be noted in the constructive and critical context of discussion on Refs [41, 42]:

1. Analytical approaches, methods, and results [6–9] of the thermodynamical and crystallochemical analyses and comparison and systematization of a large body of data [10–53] make it possible to effectively resolve at the electronic, atomic, and nanostructural levels many 'open' questions raised in Refs [1–5].

2. The analytical approaches and methods developed in Refs [6–9] provide a solution to the fundamental problem [44, 45] of adequately determining the thermodynamic properties of carbon in austenite within a framework of the quasichemical model which involves pairwise interaction with neighboring iron atoms only in the first coordination sphere of the impurity, a fact which should be taken into account when analyzing and interpreting the Mössbauer spectra of iron in austenite and martensite [15, 16, 27, 28, 41, 42, 46–50].

3. The analysis and interpretation of the Mössbauer spectra of iron in martensite [16, 27, 28, 41, 46–50] also requires using the results of the ECOPoSAP analysis [34, 52, 53] (see Fig. 3) and other relevant data, in particular, from Refs [9, 34], on carbide-like nanosegregations on dislocations (see Fig. 3) and grain boundaries. In turn, when analyzing and interpreting ECOPoSAP data [34, 52, 53] it is necessary to take into account the results of Mössbauer and other measurements, whose analysis was given in Ref. [9].

4. Further research in this area should most appropriately be done on nitrogen steels (to obtain more information and insight in light of their comparison with carbon steels).

5. The lack of satisfactory agreement between the results of the present work and those obtained in Refs [41, 42] and some other studies warrants a detailed and constructive discussion in scientific periodicals and at conferences.

7. Conclusion

The study performed shows that the process of carbon distribution in Fe–C systems in martensite transformations may be related to the spontaneous occurrence in a material of a certain quasichemical reaction in various cluster regions that form as austenite cools down and which contain original carbo-austenite (spherically symmetric) molecules comprising γ-iron and carbon atoms and octahedral γ interstices (γ-$Fe_6C(OI_\gamma)_6$).

An MT involves the local redistribution of electron density (and iron atoms) in the original γ-$Fe_6C(OI_\gamma)_6$ molecules in cluster regions on the order of the critical value in size for the onset of the MT, leading to the formation and ordering in these regions of new carbo-ferrite α-$Fe_2C(OI_\alpha)_6$ molecules containing α-iron atoms, carbon and octahedral α interstices (cylindrically symmetric and with stronger covalent Fe–C σ bonds) and a certain amount of α-iron in octahedral α interstices, and to the formation of strong local stresses necessary for the shear MT deformation of the material. This can be viewed as the quasichemical, or crystallochemical, component of the MT mechanism in carbon steels.

It is also shown that carbon steel undergoing a high-rate MT deformation may exhibit a concomitant process, induced by the martensite transformation, in which a considerable

proportion of carbon atoms is diffusively redistributed from the martensite lattice to dislocations that develop in the material and on which they form carbide-like nanosegregations — a process which is characterized by anomalously high diffusion coefficients corresponding to the craudion type mechanism.

References

1. Kurdyumov G V, Utevskii L M, Entin P I *Prevrashcheniya v Zheleze i Stali* (Transformations in Iron and Steel) (Moscow: Nauka, 1977)
2. Lobodyuk V A, Estrin E I *Martensitnye Prevrashcheniya* (Martensite Transformations) (Moscow: Fizmatlit, 2009)
3. Lobodyuk V A, Estrin E I *Usp. Fiz. Nauk* **175** 745 (2005) [*Phys. Usp.* **48** 713 (2005)]
4. Mogutnov B M *Izv. RAN Ser. Fiz.* **66** 1230 (2002)
5. Bannykh O A, in *Programma III Mezhdunar. Konf. 'Deformatsiya i Razrushenie Materialov i Nanomaterialov', Moscow, 12 – 15 Oktyabrya 2009* (Program of III Intern. Conf. 'Deformation and Destruction of Materials and Nanomaterials', 12 – 15 October 2009), p. 1
6. Nechaev Yu S, in *Tez. Dokl. na Pervykh Moskovskikh Chteniyakh po Problemam Prochnosti Materialov, Posvyashchennykh Pamyati V L Indenboma i L M Utevskogo, Moskva, 1 – 3 Dekabrya 2009* (Abstracts of Papers of the First Moscow Readings on the Problems of Material Strength, Dedicated to the Memory of V L Indenbom and L M Utevskii, Moscow, 1 – 3 December 2009), p. 126
7. Nechaev Yu S, Oechsner A, in *Abstracts of Intern. Workshop 'Grain Boundary Diffusion, Stresses and Segregation', Moscow, 1 – 4 June 2010*, p. 52
8. Nechaev Yu S, in *Tez. Dokl. IV Mezhdunar. Konf. 'Fazovye Prevrashcheniya i Prochnost' Kristallov', Posvyashchennoi Pamyati Akademika G V Kurdyumova, Chernogolovka, 16 – 19 Noyabrya 2010* (Abstracts of Papers of IV Intern. Conf. 'Phase Transformations and Strength of Crystals' dedicated to the memory of Academician G V Kurdyumov, Chernogolovka, 16 – 19 November 2010); http://www.mks-phys.ru/
9. Nechaev Yu S *Usp. Fiz. Nauk* **178** 709 (2008) [*Phys. Usp.* **51** 681 (2008)]
10. Mogutnov B M, Tomilin I A, Shvartsman L A *Termodinamika Splavov Zheleza* (Thermodynamics of Iron Alloys) (Moscow: Metallurgiya, 1984)
11. Krishtal M A *Mekhanizm Diffuzii v Zheleznykh Splavakh* (Diffusion Mechanism in Iron Alloys) (Moscow: Metallurgiya, 1972)
12. Smirnov A A *Teoriya Diffuzii v Splavakh Vnedreniya* (Theory of Diffusion in Interstitial Alloys) (Kiev: Naukova Dumka, 1982)
13. Novikov I I *Defekty Kristallicheskoi Reshetki Metallov* (Defects in the Metal Crystal Lattice) (Moscow: Metallurgiya, 1968)
14. Zvyagintsev N V, Mogutnov B M *Fiz. Met. Metalloved.* **46** 881 (1978)
15. Choo W K, Kaplow R *Acta Metal.* **21** 725 (1973)
16. Gavrilyuk V G, Nadutov V M, Gladun O V *Fiz. Met. Metalloved.* **56** (3) 128 (1990)
17. Bernshtein M L et al. *Metallovedenie i Termicheskaya Obrabotka Stali. Spravochnik* (Physical Metallurgy and the Thermal Treatment of Steel. Handbook) Vol. 2 *Osnovy Termicheskoi Obrabotki* (The Essentials of Thermal Treatment) (Eds M L Bernshtein, A G Rakhshtadt) 3rd ed. (Moscow: Metallurgiya, 1983)
18. Morinaga M et al. *J. Phys. F* **18** 923 (1988)
19. Andreev L A et al. *Phys. Status Solidi B* **163** 221 (1991)
20. Nechaev Yu S, Omel'chenko A V *Zh. Fiz. Khim.* **69** 1765 (1995) [*Russ. J. Phys. Chem.* **69** 1408 (1995)]
21. Smith R P *J. Amer. Chem. Soc.* **68** 1163 (1946)
22. Banya S, Elliot J F, Chipman J *Metallurg. Trans.* **1** (5) 1313 (1970)
23. Nechaev Yu S, Omel'chenko A V *Zh. Fiz. Khim.* **69** 1556 (1995)
24. Naka M, Masumoto J, Imai Y *Sci. Rep. Res. Inst. Tohoku Univ.* **24** (1/2) 30 (1972)
25. Omel'chenko A V, Soshnikov V I, Bashchenko A P *Izv. Akad. Nauk SSSR. Metally* (1) 190 (1991)
26. Sychev V V, Vasserman A A, Kozlov A D *Termodinamicheskie Svoistva Azota* (Thermodynamic Properties of Nitrogen) (Moscow: Izd. Standartov, 1977) p. 250
27. Gavriljuk V G *ISIJ Int.* **36** 738 (1996)
28. Gavrlljuk V G, Shanina B D, Berns H *Acta Mater.* **48** 3879 (2000)
29. Nechaev Yu S, Efimenko S P *Metallofiz. Noveishie Tekhnol.* **21** (2) 16 (1999); *Met. Phys. Adv. Technol.* **19** (2) 225 (2001), reprint
30. Wells C, Batz W, Mehl R F *Trans. Met. Soc. AIME* **188** 535 (1950)
31. Marder A R et al. *Metallurg. Trans. A* **16** 1160 (1985)
32. Zhukhovitskii A A, Shvartsman L A *Fizicheskaya Khimiya* (Physical Chemistry) 4th ed. (Moscow: Metallurgiya, 1987)
33. Blanter M S et al. *Internal Friction in Metallic Materials. A Handbook* (Berlin: Springer-Verlag, 2007)
34. Wilde J, Cerezo A, Smith G D W *Scripta Mater.* **43** 39 (2000)
35. Novikov I I, Stroganov G B, Novikov A I *Metallovedenie, Termoobrabotka i Metallografiya* (Physical Metallurgy, Thermal Treatment and Metallography) (Moscow: MISIS, 1994)
36. Nechaev Yu S *Diffusion Defect Forum* **251 – 252** 123 (2006)
37. Mazanko V F, Pokoev A V, Mironov V M *Diffuzionnye Protsessy v Metallakh pod Deistviem Magnitnykh Polei i Impul'snykh Deformatsyi* (Diffusion Processes in Metals under Magnetic Fields and Pulsed Deformations) Vol. 1 (Moscow: Mashinostroenie, 2006)
38. Indenbom V L *Pis'ma Zh. Eksp. Teor. Fiz.* **12** 526 (1970) [*JETP Lett.* **12** 369 (1970)]
39. Chilton J M, Kelly P M *Acta Metallurg.* **16** 637 (1968)
40. Kehoe M, Kelly P M *Scripta Metallurg.* **4** 473 (1970)
41. Sozinov A L, Balanyuk A G, Gavriljuk V G *Acta Mater.* **45** 225 (1997)
42. Bol'shov L A, Suslov V N *Fiz. Met. Metalloved.* **98** (6) 3 (2004) [*Phys. Met. Metallogr.* **98** 547 (2004)]
43. Hirth J P, Lothe J *Theory of Dislocations* (New York: McGraw-Hill, 1968) [Translated into Russian (Moscow: Atomizdat, 1972)]
44. Alex K, McLellan R B *Acta Metallurg.* **19** 439 (1971)
45. Alex K, McLellan R B *Acta Metallurg.* **20** 11 (1972)
46. Gielen P M, Kaplow R *Acta Metallurg.* **15** 49 (1967)
47. Ino H et al. *Acta Metallurg.* **30** 9 (1982)
48. Kaplow R, Ron M, DeCristofaro N *Metallurg. Trans. A* **14** 1135 (1983)
49. Taylor K A, Cohen M *Prog. Mater. Sci.* **36** 151 (1992)
50. Olson G B, Cohen M *Metallurg. Trans. A* **14** 1057 (1983)
51. Nagakura S et al. *Metallurg. Trans. A* **14** 1025 (1983)
52. Peet M et al. *Scripta Mater.* **50** 1277 (2004)
53. Miller M K et al. *Metallurg. Trans. A* **14** 1021 (1983)